

SUPPLEMENTARY INFORMATION

Structural determinants of a permeation barrier of the SecYEG translocon in the active state

Ekaterina Sobakinskaya,^{*a} Heinrich Kroboth,^a Thomas Renger^a and Frank Müh^a

^a Institute for Theoretical Physics, Johannes Kepler University Linz, Altenberger Strasse 69, A-4040
Linz, Austria.

** E-mail: ekaterina.sobakinskaya@jku.at.*

ESI Tables

Table S1 Charged amino acids residues, located above the PR in the translocon channels of different organisms (indicated by the respective PDB ID).

Archaea		Bacteria			Eukaryotes
1RHZ <i>M. jannaschii</i>	3MP7 <i>P. furiosus</i>	5AWW <i>T. thermophilus</i>	3DIN <i>T. maritima</i>	5GAE <i>E. coli</i>	3J7R <i>S. scrofa</i>
Arg 413 Asp 158	Arg 445	Asp 410	Asp 404	Asp 399	–

ESI Figures

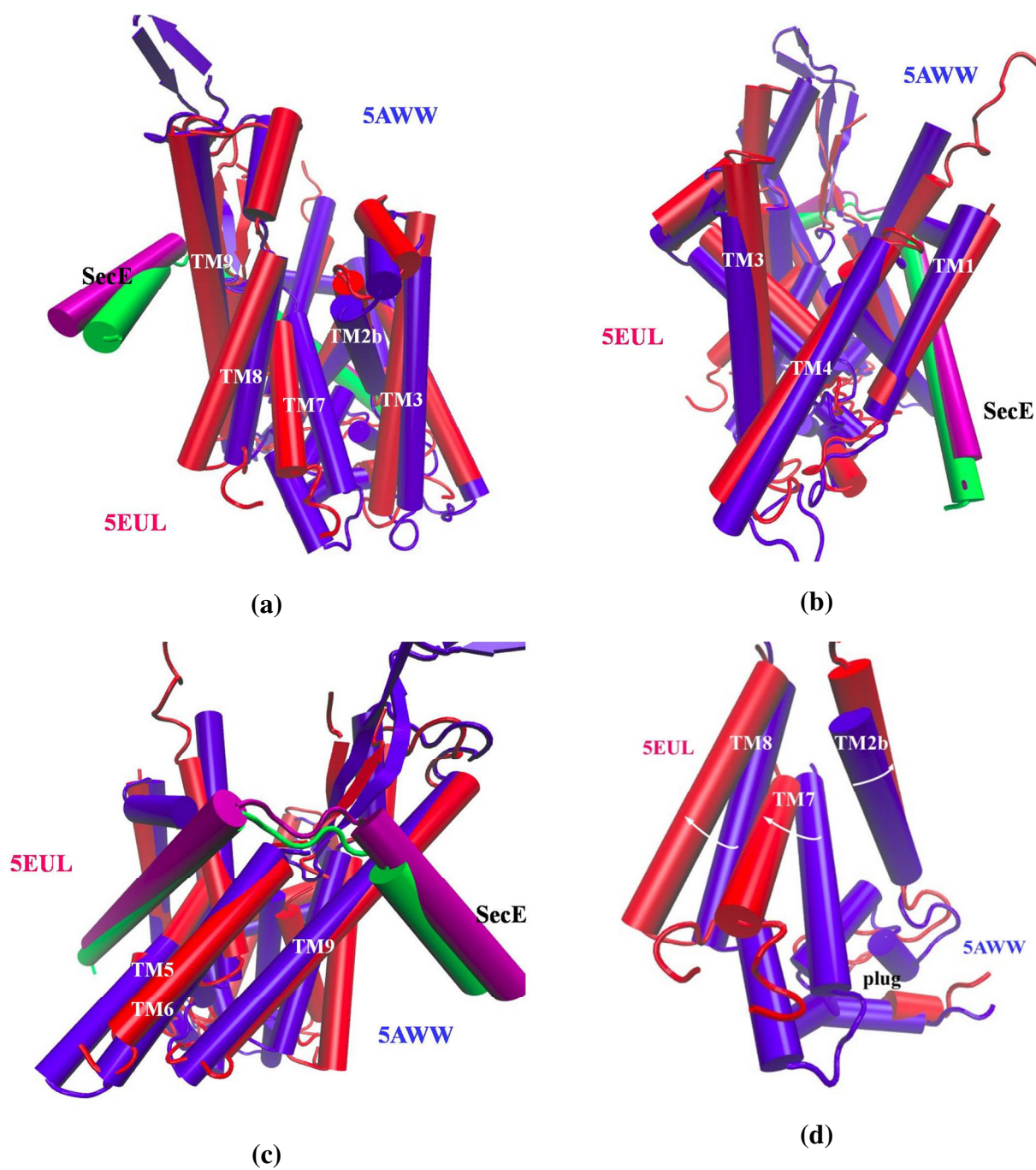


Fig. S1 Overlay of the crystal structures 5AWW (blue color) and 5EUL (red color). The views in (a), (b), and (c) are all along the membrane plane and differ in orientation. White arrows in (d) indicate the direction of pulling for TM2, TM7, and TM8 of 5AWW to open the LG.

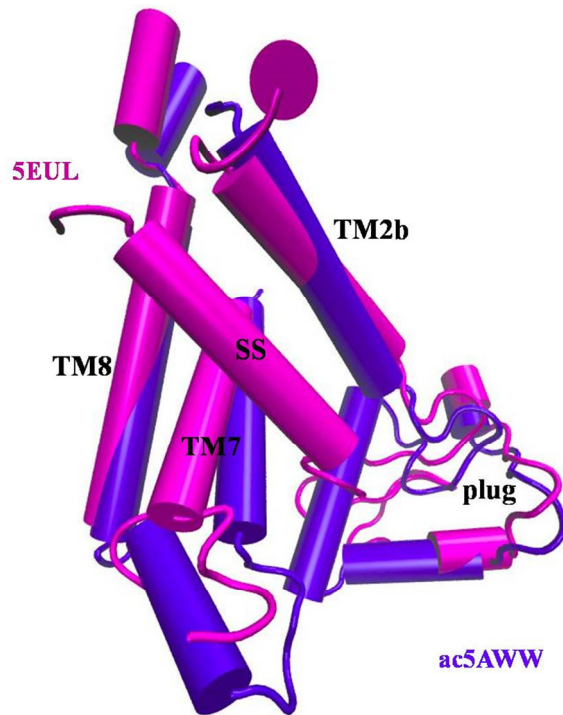


Fig. S2 Overlay of the active channel with open lateral gate, ac5AWW, with the crystal structure 5EUL. Only helices TM2b, TM7, and TM8 as well as the SS and the plug are shown.

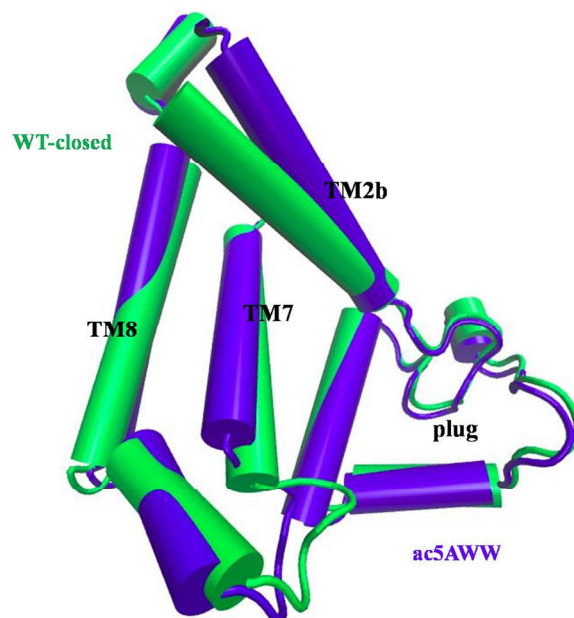


Fig. S3 Comparison of the WT-closed setup, after equilibration, with ac5AWW. Only helices TM2b, TM7, TM8 and the plug are shown.



Fig. S4 Comparison of the WT-closed setup, after equilibration, with the crystal structure 5EUL. **(a)** Complete backbone architecture. **(b)** Only helices TM2b, TM7, TM8 and the plug are shown. Color code: SecY of 5EUL, red; SecY of WT-closed, blue; SecE of 5EUL, magenta, SecE of WT-closed, green; SS of 5EUL, yellow, SS of WT-closed, orange.

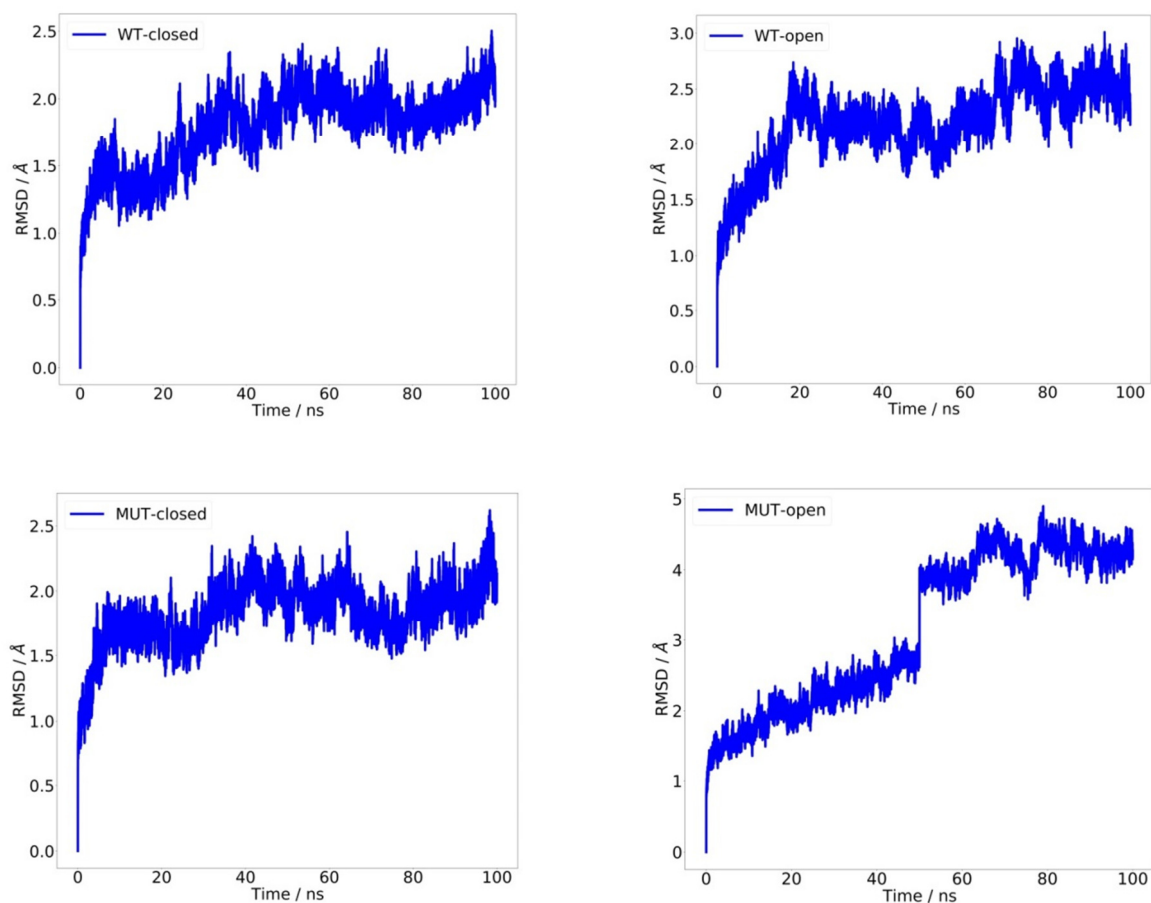


Fig. S5 RMSD of the translocon's backbone relative to the starting conformation for the unbiased 100-ns MD simulations trajectories. To obtain reliable data for the fluctuations of helix positions, we excluded from the RMSD computations the N- and C-terminus (residues 1 to 10 and 427 to 444) as well as a long and flexible linker (residues 238 to 269). Additionally, for the setups WT- and MUT-open, we excluded the plug from the selection, since it is highly flexible in the open state. One can readily see that the setups with an open plug reveal stronger fluctuations in both WT and MUT.

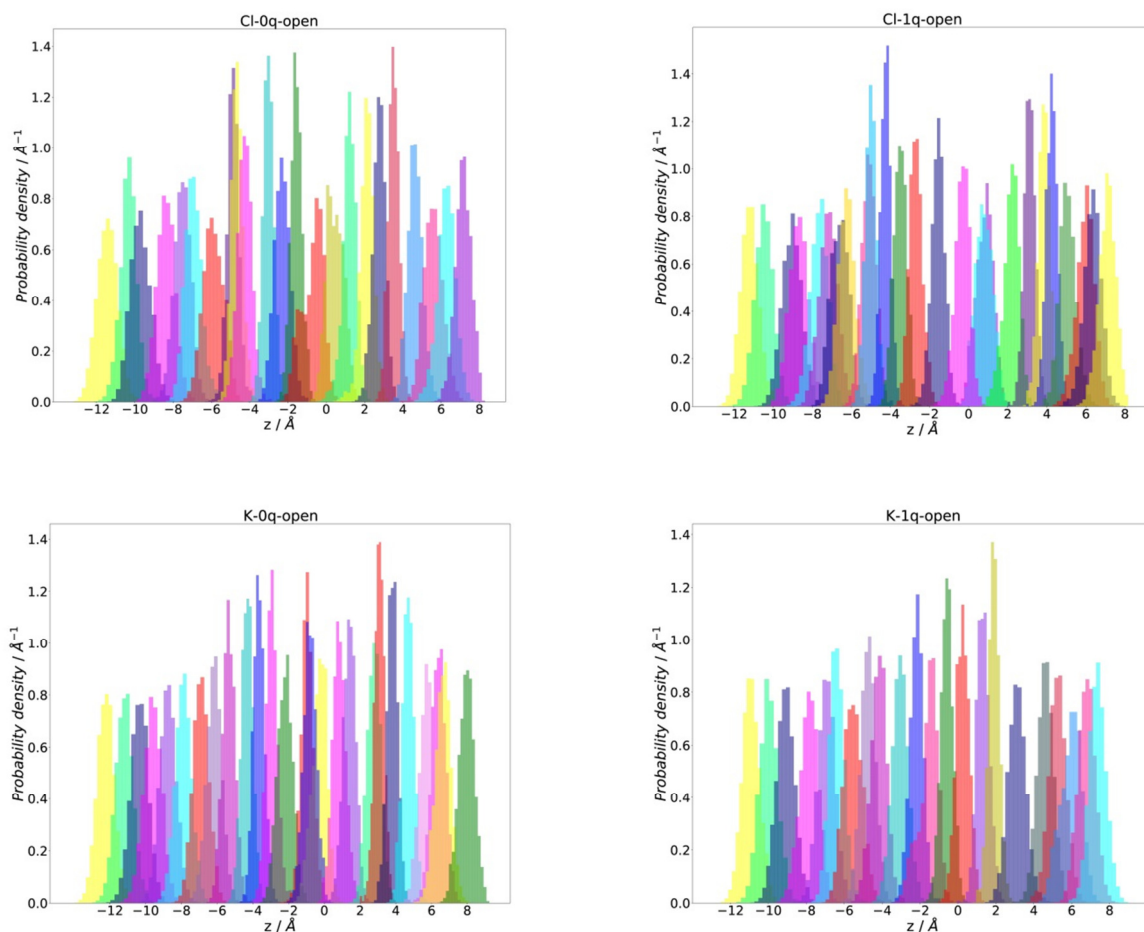


Fig. S6 Probability density functions of US sampling for all setups: Different colors correspond to individual windows.

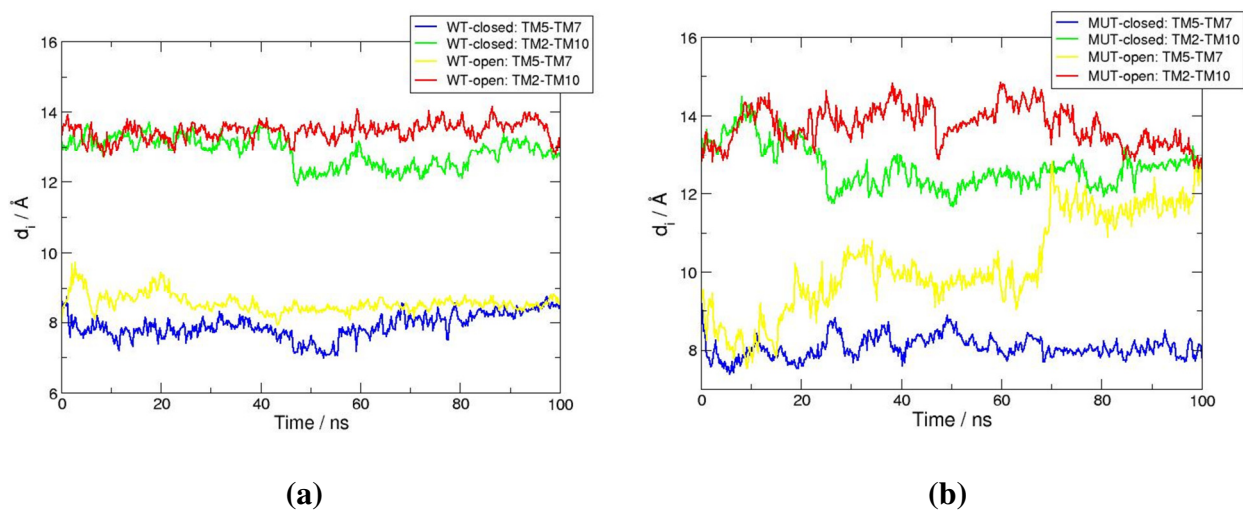


Fig. S7 Time dependence of the pore ring diameter for WT **(a)** and MUT **(b)** setups.

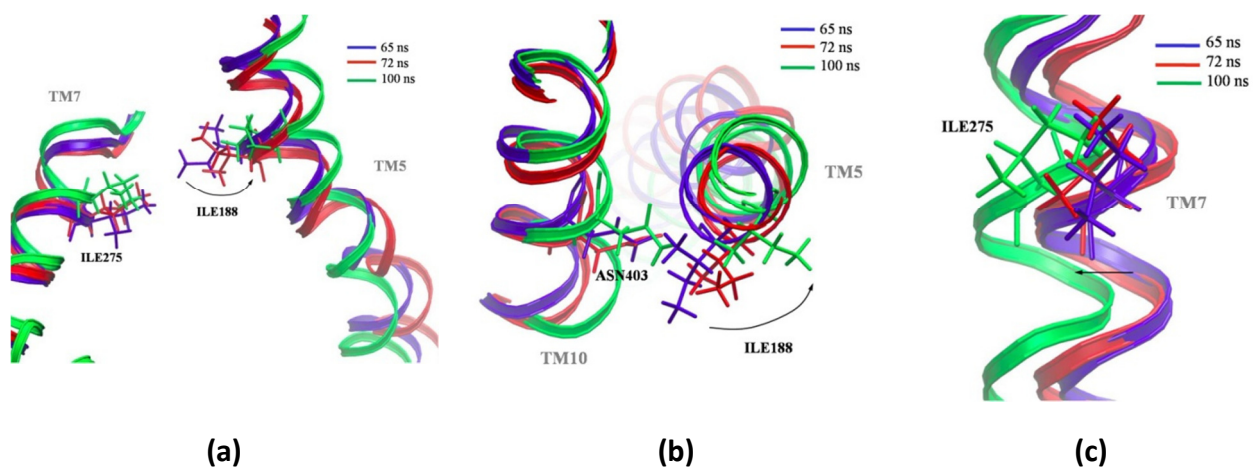


Fig. S8 Snapshots of the MUT-open setup at 65, 72, and 100 ns around the conformational switch. Shown are (a) the two PR residues Ile 188 (TM5) and Ile 275 (TM7), (b) Ile 188 (TM5) and the mutated Asn 403 (TM10), as well as (c) the movement of TM7.

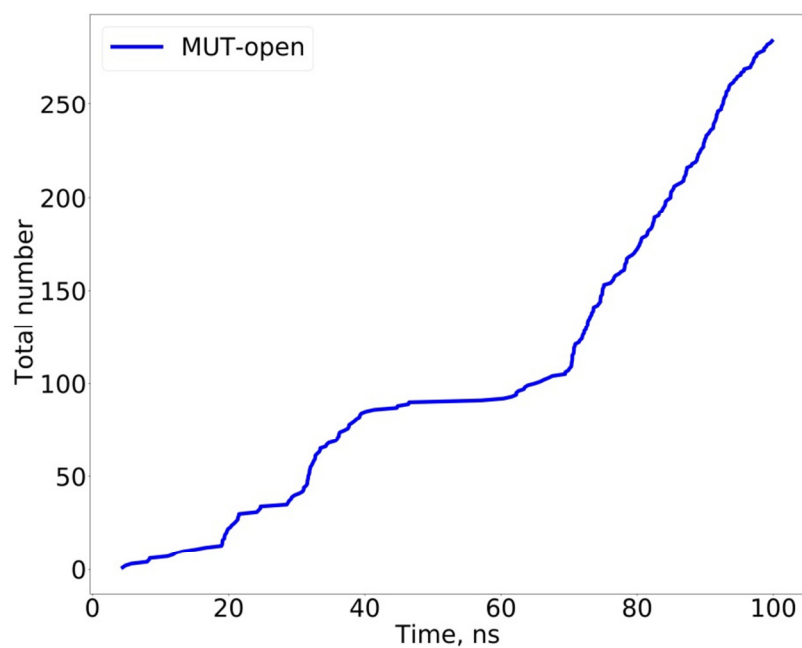


Fig. S9 Total number of water molecules crossing PR in both directions as a function of time. The step increase of water crossings starting at 70 ns coincides with the conformational transition associated with 2 Å distance increase between TM5-TM7 (see Fig.S7).

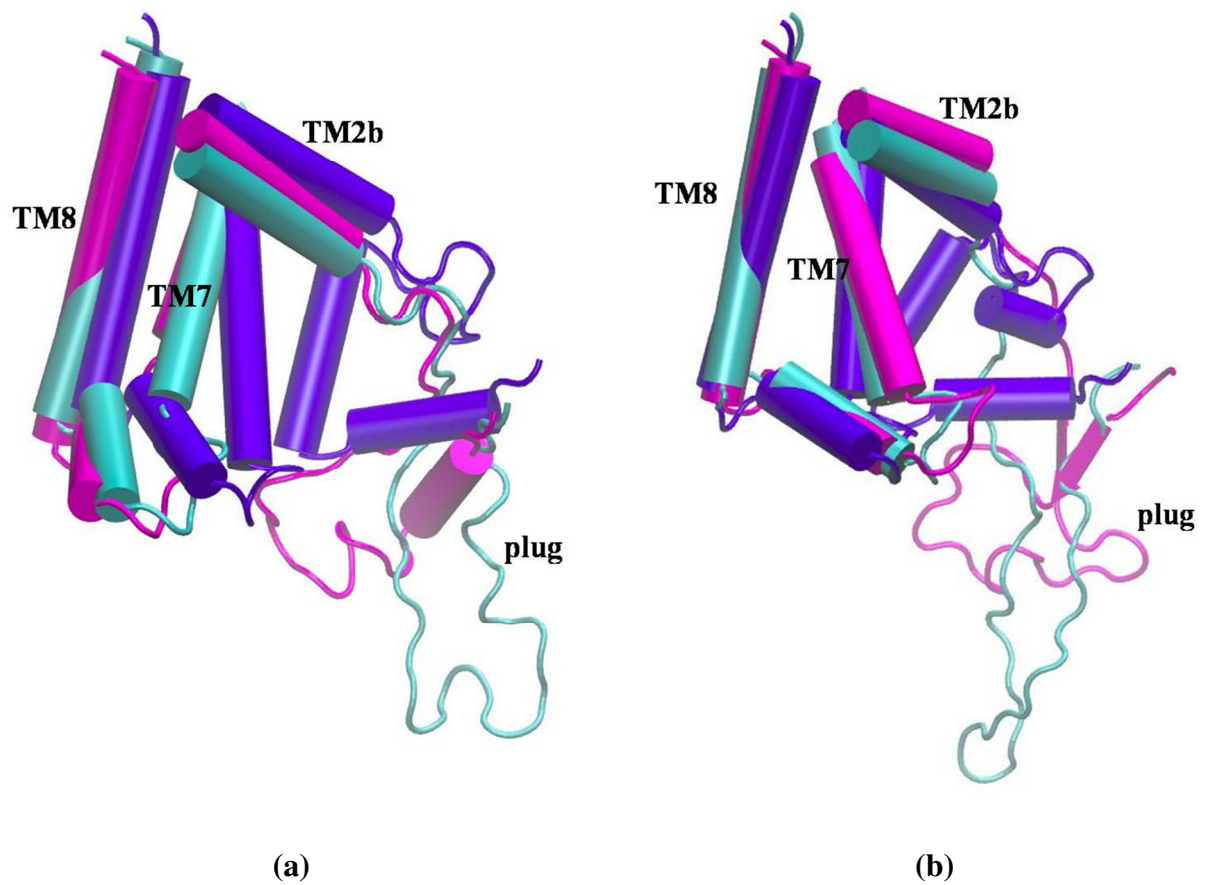


Fig. S10 Comparison of the plug position and conformation for the WT (a) and MUT (b) setups. SecYEG with closed plug is depicted in blue. SecYEG with open plug in the beginning of the dynamics is colored in cyan and in magenta at the end of the MD simulations. Only TM2b, TM7, TM8, and plug helices are shown.

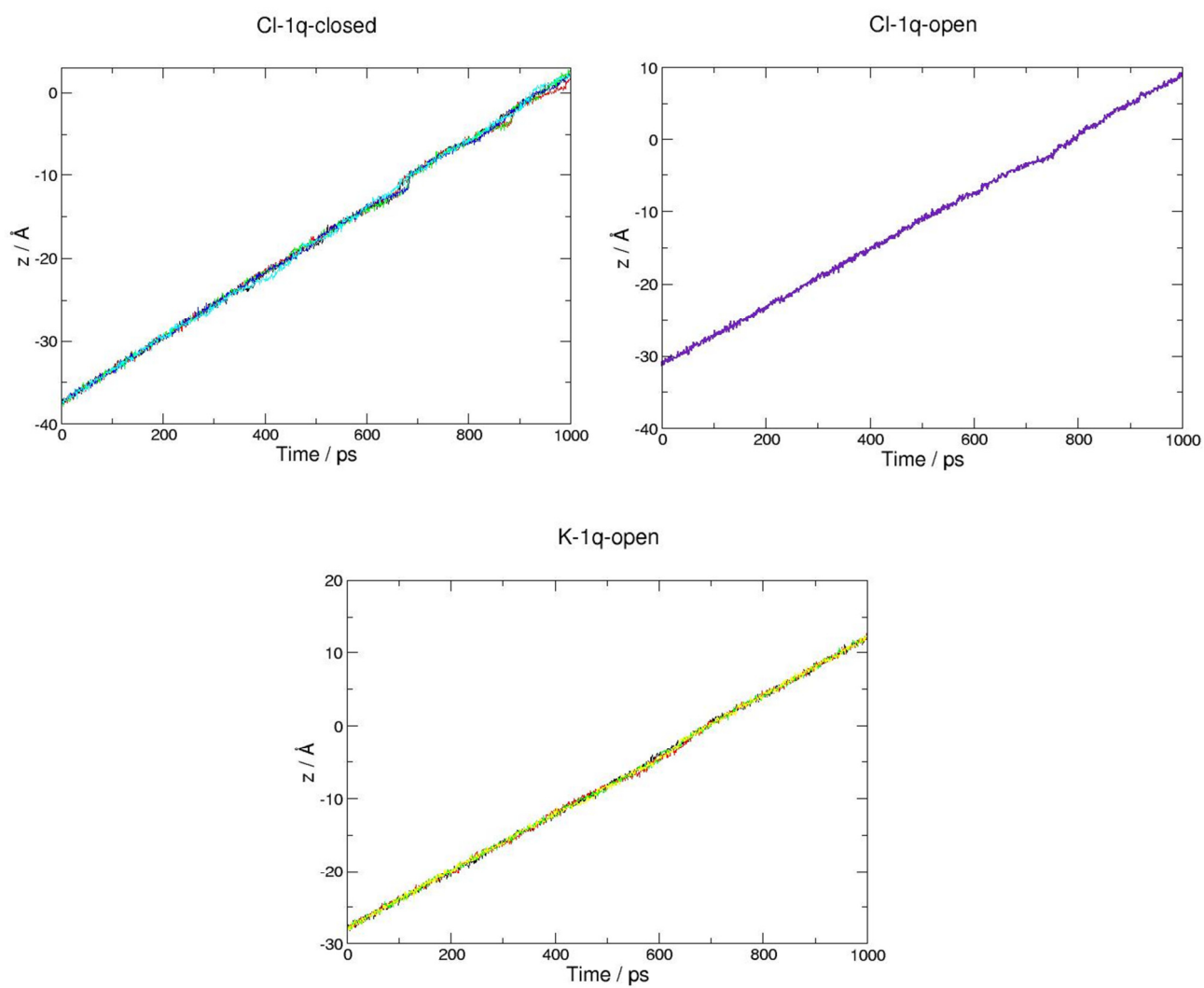


Fig. S11 Time dependence of the ion position (z -coordinate) in the SMD simulations. Coordinates from five arbitrarily chosen trajectories are shown for each setup.

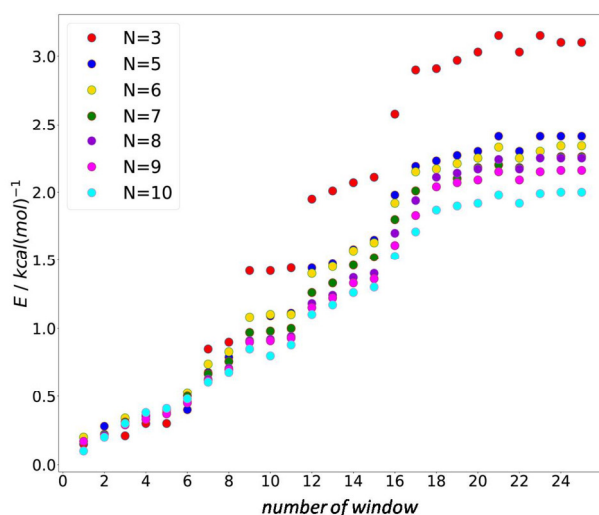


Fig. S12 The dependence of the PMF errors, E , on block number N for all windows of the case Cl-1q-open.

Calculation of error bars: The errors were calculated with the method described in **F. Zhu, G. Hummer, J. Comput. Chem. 2012, 33, 453-465**. The important parameter of the approach is the number of the blocks, N , into which every trajectory is divided. For practical applications, N is chosen between 5 and 10. In our case, we have used $N = 7$. There is a very small variation of the magnitude of E in the range from 5 to 10. In contrast, for $N = 3$, the errors are much higher.

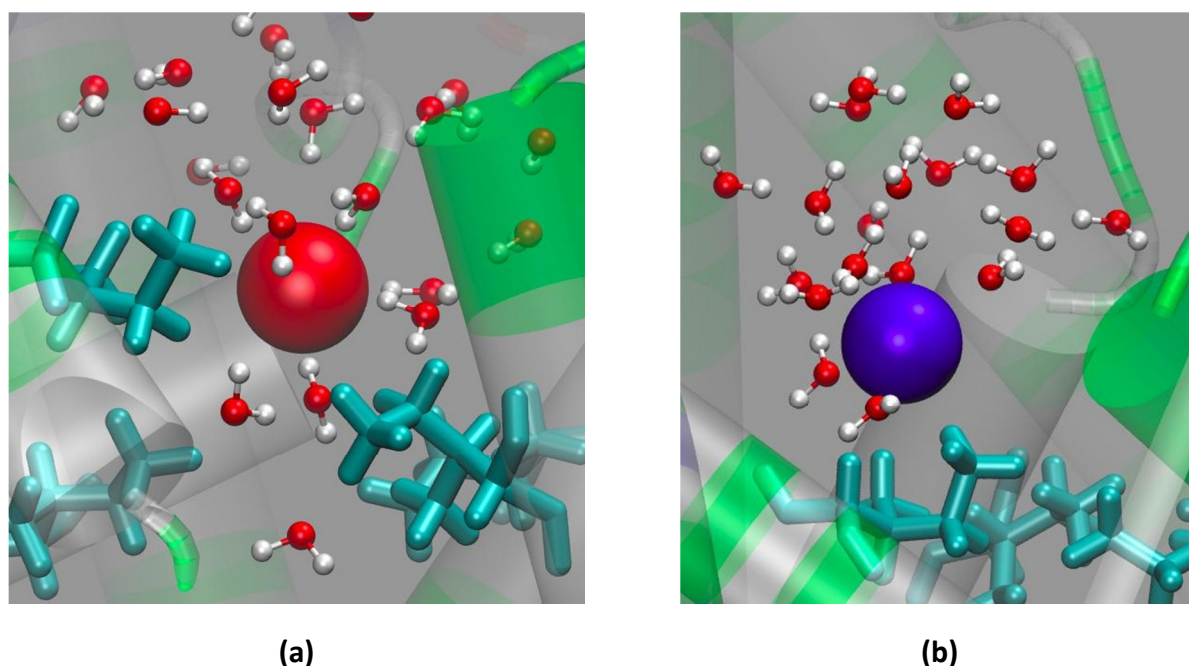


Fig. S13 Illustration of the different orientation of the water molecules, located within 7 \AA of the ions near the PR area: (a) Cl^- at the distance $z = -0.9 \text{ \AA}$ in Cl-1q-open setup, (b) K^+ at the distance $z = -1.2 \text{ \AA}$ in K-1q-open setup. Snapshots are taken at the time frame corresponding to 40 ns of the MD trajectory. Cl^- and K^+ ions are depicted with red and blue balls, respectively. Pore ring residues are explicitly shown and colored in cyan. Helices of SecY are given in cartoon representation and colored according to the residue type (grey, hydrophobic; green, polar; blue, positively charged; red, negatively charged).

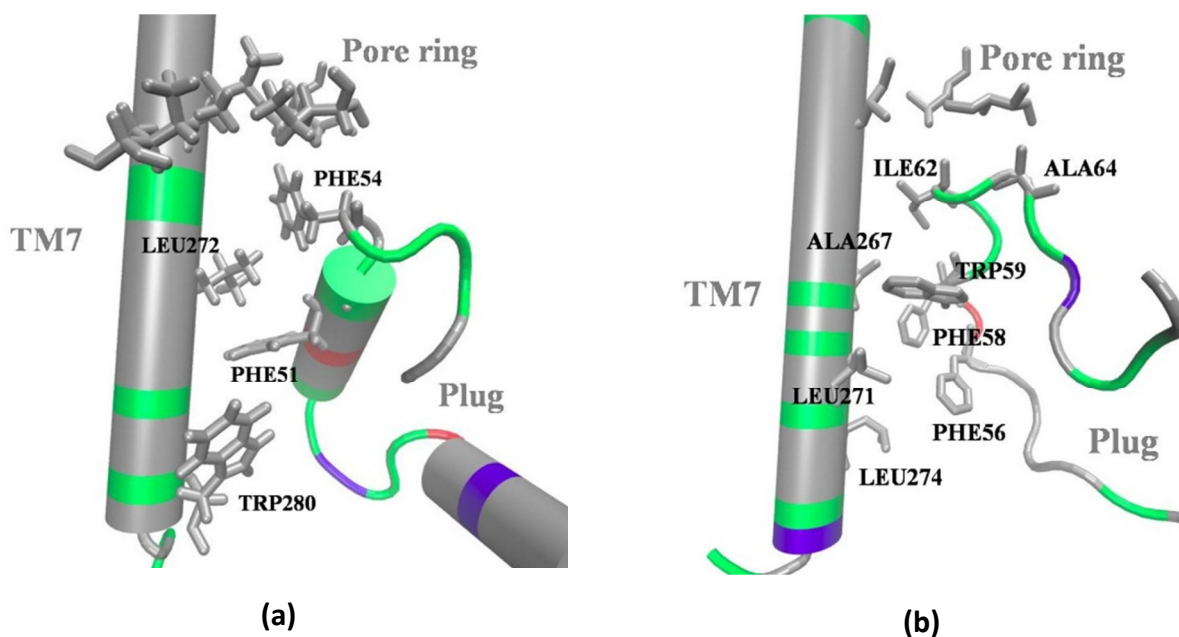


Fig. S14 Hydrophobic interactions between TM7, plug and pore ring in (a) *E. coli* (PDB ID 5GAE) and (b) *Methanocaldococcus jannaschii* (PDB ID 1RH5). Color code for amino acid types: grey, hydrophobic; green, polar; blue, positively charged; red, negatively charged (the latter two in the standard protonation state). Hydrophobic residues in close proximity are explicitly shown.

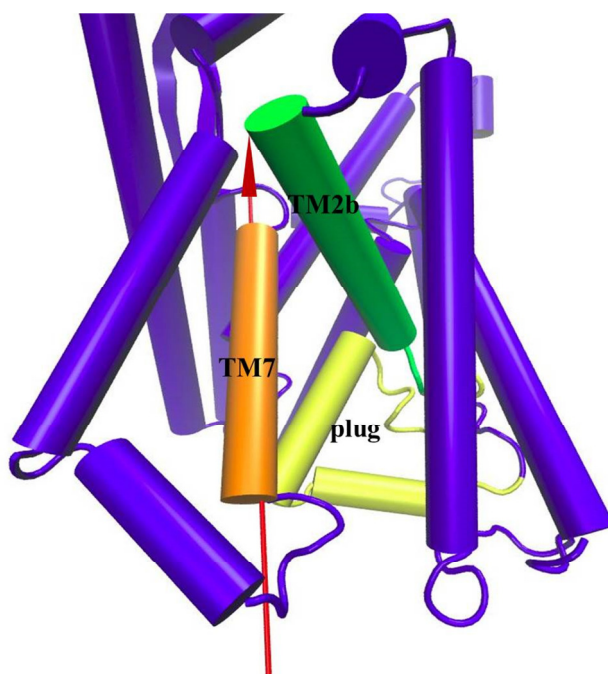


Fig. S15 Visualization of the dipole moment (red arrow) of TM7 as given by VMD. Its direction coincides almost with the helix axis and makes an angle of 56° with the z -axis defining the membrane normal.

ESI Text

T1 Description of the independent-samples t-test used to analyze averaged interaction energies.

We used the Shapiro-Wilk test to demonstrate that most of our datasets for interaction energies computed from Traj1 and Traj2 (cf. main text) can be satisfactorily described by a normal distribution. A test of outliers, using boxplots, revealed the presence of up to 6 data points that were more than 1.5 box-lengths apart for some trajectories. This result can be due to limits of the Shapiro-Wilk test, which is usually used for samples containing only up to 50 data points. However, it was proved for every case that removing outliers did not influence the mean differences and standard deviations significantly and did not change p -values. Also, in a few cases, removal of the outliers helped to improve the normal distribution, making the results of the t-test more reliable. For such cases, we present the results obtained with outliers removed. Equality of variances was evaluated by using Levene's test. For those trajectories, where the equality of variances was violated, the results of the modified (Welch's) t-test are given.

The results of the t-test for all trajectories demonstrated statistically significant differences between means (statistical significance $p < 0.05$), and therefore, we can reject the null hypothesis (same mean for Traj1 and Traj2) and accept the alternative hypothesis (mean values are different for Traj1 and Traj2).